Science of the Total Environment 998 (2025) 180230

Contents lists available at ScienceDirect

Science of the Total Environment

journal homepage: www.elsevier.com/locate/scitotenv

Multidecadal water quality trends across 15 European river basins along a Mediterranean climate gradient

Diogo Costa [a,b,c,*], Jian Liu [d], Patricia Palma [b,e,f]

[a] MED – Mediterranean Institute for Agriculture, Environment and Development & CHANGE – Global Change and Sustainability Institute, Departamento de Geociências, Escola de Ciências e Tecnologia, Universidade de Évora, Pólo da Mitra, Ap. 94, 7006-554 Évora, Portugal
[b] Center for Sci-Tech Research in Earth System and Energy (CREATE), Universidade de Évora, 7000-671 Évora, Portugal
[c] Department of Geography and Planning, University of Saskatchewan, 105 Administration Pl, Saskatoon, SK S7N 5A2, Canada
[d] The Norwegian Institute of Bioeconomy Research (NIBIO), P.O. Box 115, 1431 Ås, Norway
[e] GeoBioTec, NOVA School of Science and Technology, Campus da Caparica, 2829-516 Caparica, Portugal
[f] Department of Technologies and Applied Sciences, Polytechnic Institute of Beja, R. Pedro Soares S/N, 7800-295 Beja, Portugal

HIGHLIGHTS

- Water quality data analyzed for 14 Mediterranean basins between 1990 and 2024
- Strong north-south variability linked to climate gradient and land use/cover
- Basins within farmland had higher NO_3 and P_2O_5, and low DO and transparency in water.
- Clear shift after 2005, with nutrients increasing mostly due to drought and farming

GRAPHICAL ABSTRACT

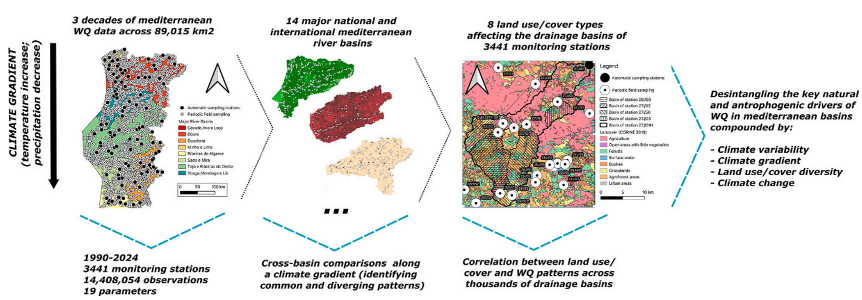

ARTICLE INFO

Keywords:
Water quality
Historical monitoring
Watersheds
Mediterranean regions

ABSTRACT

Water quality degradation is a major issue in Mediterranean regions, but identifying the key natural and human drivers remains challenging, requiring large–scale studies for meaningful synthesis and comparison. This study analyzed a vast Mediterranean dataset spanning 89,015 km^2 across 15 Iberian river basins along a climate gradient (cooler-wetter north to warmer-drier south), 3 decades, 3441 stations, 19 parameters, and ∼15 million observations. It is the first study of this scale in the region, utilizing custom scripts for automated data compilation and processing.

The study revealed an evident north–to–south water quality decline, with rising electric conductivity, pH, total suspended solids, nitrogen, phosphorus, organic carbon, and sulphate, alongside reduced dissolved oxygen and transparency. This pattern correlated with the latitudinal climate gradient and intensified agriculture in the south (Pearson correlation coefficient: 0.1 to 0.53; Spearman's rank correlation coefficient: 0.17 to 0.56), while increased forest cover had a mitigating effect (Pearson: −0.50 to −0.07; Spearman: −0.51 to −0.10). Multidecadal trend analysis revealed a shift around 2005 with most parameters decreasing, except for nitrate and phosphate, which rose likely due to the 2004/05 drought reducing river dilution and expanded irrigated agriculture, especially in Alentejo with the Alqueva reservoir.

* Corresponding author at: MED – Mediterranean Institute for Agriculture, Environment and Development & CHANGE – Global Change and Sustainability Institute, Departamento de Geociências, Escola de Ciências e Tecnologia, Universidade de Évora, Pólo da Mitra, Ap. 94, 7006-554 Évora, Portugal.
E-mail address: diogo.costa@uevora.pt (D. Costa).

https://doi.org/10.1016/j.scitotenv.2025.180230
Received 4 September 2024; Received in revised form 4 August 2025; Accepted 6 August 2025
Available online 22 August 2025

These findings are crucial for guiding future national management actions and pollution reduction initiatives in Mediterranean regions, aligning with the European Commission's "European Green Deal" that targets a 50 % reduction in nutrient losses to make agriculture more environmentally sustainable, and also provide a valuable reference to many other regions with similar challenges for water quality management.

1. Introduction

Many aquatic ecosystems across Europe face significant water quality issues, particularly from excess nutrients and eutrophication (Costa et al., 2022). Despite decades of EU efforts, such as the Nitrates Directive, Urban Waste Water Treatment Directive, and Water Framework Directive, nitrogen (N) and phosphorus (P) pollution remain a problem. By 2020, Europe's N and P losses exceeded safe limits by 3.3 and 2 times, respectively, with around 36 % of rivers, 32 % of lakes, and 80 % of coastal waters considered eutrophic (EEA and FOEN, 2020). Nitrate (NO_3) concentrations in groundwater have remained stable since 2000 with concentrations averaging 21 mg/L. About 14 % of the monitoring stations show concentrations exceeding the 50 mg/NO_3 threshold for human consumption and they are mainly located in northern-central and southern–western Europe (EC, 2021, particularly Figs. 2 and 4). EC (2021). Between 2012 and 2015 and 2016–2019, the total area considered polluted and eutrophic across all EU member states has increased by 14 % (EC, 2021). Nitrogen emissions into the atmosphere from agriculture through mainly animal husbandry and fertilizer use are estimated to cost Europe almost €400 billion annually in health and economic impacts (Giannadaki et al., 2018). The EU's Green Deal now aims to cut nutrient losses by 50 % by 2030.

Climate change is expected to worsen water quality issues globally (Costa et al., 2022), with Mediterranean regions becoming particularly vulnerable to nutrient leaching and material transport due to more frequent extreme precipitation events (Schlingmann et al., 2020). Seasonal changes in streamflow will follow shifts in precipitation patterns, but the impacts on hydrology and nutrient dynamics will vary by region (Costa et al., 2022). In erosion-prone areas such as eastern Norway, extreme rainfall is exacerbating nutrient loading (Confesor et al., 2023). The Mediterranean climate is characterized by dry, hot summers and cool, rainy winters; however, higher temperatures are projected in the future, increasing the likelihood of harmful cyanobacterial blooms by enhancing thermal stratification, increasing nutrient influx, and reducing summer flow, especially during droughts (Radbourne et al., 2020).

The rapid expansion of agricultural and urban land further exacerbates the challenge, increasing threatens to freshwater health. Certain Mediterranean regions like Portugal, for example, are particularly vulnerable, as they are downstream major transboundary river systems, in this case shared with Spain. About 78 % of the river basins located upstream in Spain, making Portugal susceptible to diffuse pollution. Agriculture occupies nearly 50 % of the Iberian Peninsula (Fernández-Nogueira and Corbelle-Rico, 2018), with 42.3 % of Portugal's and 52.3 % of Spain's land use/land cover (LULC) used for farming (World-Bank, 2024). Intensive farming practices have risen from 11.9 % in 2005 to 14.5 % in 2018. Urban areas have also expanded, with urban populations in 2021 reaching 66.85 % in Portugal and 81.06 % in Spain (World-Bank, 2024).

Studies of water quality of major Mediterranean river systems and reservoirs remain largely individualized on specific systems. For example, in Portugal focus has been given to the Alqueva Reservoir (Raposo et al., 2022; Rodrigues et al., 2020; Neves et al., 2021; Alves-Ferreira et al., 2024), Aveiro Lagoon (Vale, 2023; Lopes et al., 2019), Ria Formosa (Cravo et al., 2019; Rodrigues et al., 2021), Tagus (Franz et al., 2014; Silva et al., 2012), Douro (Azevedo et al., 2008; Cabecinha et al., 2009) and Guadiana (Company et al., 2008; Palma et al., 2021) Rivers. Particular emphasis has been given to the effect of urban pollution (Almeida et al., 2021; Teixeira et al., 2020), eutrophication arising from agricultural nutrient export (Bellém et al., 2013; Vieira et al., 2013), and pesticide contamination (Alves-Ferreira et al., 2024; Palma et al., 2021). More recently, some focus has been put into understanding the impact of wildfires on water quality (Vidal et al., 2021; Serpa et al., 2020).

However, large-scale water quality studies that provide integrated and comparative analysis of different river systems are rare, not only in Mediterranean regions but also across Europe and globally. In Portugal, which encompasses 15 major Mediterranean basins, there are very few examples. For instance, Pacheco and Sanches Fernandes (2016) examined environmental land-use conflicts in 85 small agricultural watersheds (each with over 50 % agricultural land) and found NO_3 concentrations along the Atlantic coast beyond the legal limit of 50 mg/L imposed by the European and Portuguese laws. These were linked to factors such as larger population densities ($>$ 100 $Hab.Km^{-2}$), incomplete sewage coverage, and deficient wastewater treatment (see Fig. 1 in Pacheco and Sanches Fernandes (2016)). Santos et al. (2013) studied the northern transboundary Minho River, finding generally good water quality, with Biological Oxygen Demand (BOD_5) below 5 mg/L, Kjeldahl Nitrogen (KN) below 2 mg/L, and Total Phosphorus (TP) below 1 mg/L. However, the Valença and Louro sub-systems in Spain were the most polluted, with Louro being the worst with maximum observed concentrations of 26 mg/L for TSS, 6.6 mg O_2 for BOD_5, 20.8 mg O_2/L for COD, and 9.9 mg N/L for TN. Further south, Catarino et al. (2024) assessed the Lage Reservoir in the Alqueva hydro-agricultural system, finding BOD_5 values exceeding the limits for excellent ecological potential, reaching 10 mg/L during dry periods, and TN concentrations mostly above good ecological thresholds ($0.96 \leq TN \leq 2.44$ mgN/L).

While this focus on specific systems has allowed to deepen our knowledge on a variety of regional water quality problems, large-scale multi-basin comparative studies are needed to provide broader integrated evaluations of cross-regional and climate drivers. The research herein aims to reduce this research gap by examining surface water quality patterns across a Mediterranean area of 89,015 km^2 (entire country of Portugal), covering 15 major national and international river basins. The goal is two fold: (1) identifying key cross-regional patterns and drivers across this large Mediterranean region and (2) advancing methodological approaches for deadling with large water quality datasets across large domains that often comprise observations with variable sampling frequencies. The findings are relevant to other European Mediterranean regions, such as Spain, Italy, Greece, South of France, but also North of Africa and other regions around the globe with similar climates, such as California, Chile, South Africa, Southwest Australia, and northern China. To achieve this goal, the research used a unique extensive water quality dataset that spans across 3 decades and multiple Mediterranean river basins.

2. Materials & methods

2.1. Long-term dataset (1990–2024)

The dataset used is derived from the nationwide database repository managed by the Portuguese Environment Agency (APA). The National Water Resources Information System (SNIRH) makes it publicly available. This is a large unique dataset, which required the development of scripts for automating data compilation and processing since SNIRH's server allows only a maximum of 50 station–parameter combinations per download, which likely largely contributes to the lack of studies at such scales in this region. The complete dataset is available through SNIRH's website and the analysis performed in this study is available through a ZENODO database: zenodo.org/records/13971004. The repository also includes (a) all the scripts developed for this research (data extraction, compilation, and processing), (b) the figures generated provided in interactive HTML format, (c) the basin delineations of all the stations in *gkpg* format, and (d) basin-landuse intercept areas used to determine correlations between the different parameters and LULC types. The algorithms develop to extract data from SNIRH are also available at github.com/ue-hydro/eyedrop_data_extract.

In this study, we used the water quality sub-dataset for surface water, including rivers or small streams, lakes and reservoirs. It consists of observations since 1990 from a total of 3441 stations or sampling locations (in the case of point measurements). The database contains over 756 parameters, including physico-chemical support parameters, potentially toxic metals, organic compounds, and microbiological parameters. However, in this study, we focused on a sub-set of 19 parameters totalling 14,408,054 observations as shown in Table 1.

The selection of parameters was based on the following criteria: (a) their relevance to the study objectives, with a focus on parameters that enable a preliminary assessment of water quality status and trends over the past 34 years, including variability across different basins; (b) their capacity to indicate agricultural contamination, particularly those sensitive to meteorological variability and relevant to eutrophication processes; and (c) the availability of sufficient spatial and temporal data coverage, ensuring robust and meaningful analysis across multiple basins.

Fig. 1 presents the locations of all observation stations across the river basins, along with the land use and land cover (LULC) classification based on CORINE 2018 (Feranec, 2016). To improve the interpretability of results and align with the approach commonly adopted by national and European agencies (e.g., the European Environment Agency), the 15 river basins were grouped into 8 larger regional units. In this grouping, smaller basins were integrated into adjacent, larger river systems: Minho and Lima (Group 1), Cávado, Ave, and Leça (Group 2), Douro (Group 3), Vouga, Mondego, and Lis (Group 4), Tejo and Ribeiras do Oeste (Group 5), Sado and Mira (Group 6), Guadiana (Group 7), and Ribeiras do Algarve (Group 8). The map shows that the water quality monitoring stations are well distributed across the country, providing a solid basis for spatial assessment and the identification of regional trends. This spatial coverage is particularly important given the variation in sampling frequency between automatic monitoring stations and field campaigns, as detailed in Table 1.

While interactions with groundwater systems may be important for understanding particular surface water quality patterns, our focus was the surface component only. Mediterranean rivers are characterized by flashy hydrological responses, so the contribution of groundwater is frequently reduced. Yet, future research should include disentangling the contribution of surface water-groundwater (SW–GW) interactions.

2.2. Methodology

The following methodology was applied to all 19 parameters listed in Table 1. While the full set of results is available in the ZENODO repository, only a selection is presented here for clarity. Parameters were chosen based on (1) the robustness and consistency of observed trends, and (2) the size and representativeness of datasets across basins to support regional comparisons. Geographic data were sourced from OpenStreetMap (Bennett, 2010).

2.2.1. Multi-basin patterns along a climate gradient

The study basins span a north–south Mediterranean climate gradient. To assess cross-regional patterns, water quality data were grouped by basin and summarized using median concentrations. These were sorted by latitude and visualized through maps and boxplots (showing min, max, and 25th, 50th, and 75th percentiles). Given the dataset size, point-level quality control was not feasible. Medians and percentiles were used in place of means to minimize sensitivity to outliers. Stations vary in operation periods, measurement frequency, and dataset size (see Table 1); scatter plot circle sizes reflect data volume, highlighting more robust datasets.

Seasonal variation was assessed by separating data into wet (October–April) and dry (May–September) seasons. Boxplots across the latitudinal gradient depict the interplay of climate and seasonality. To explore long-term trends, data were grouped in 5–year intervals from 1990 to 2024, with the last interval covering 2020—2024. Results, stratified by parameter and basin, support comparison across the Mediterranean context.

An autocorrelation analysis has been performed and shown in Appendix A for all 19 water quality parameters across multiple time lags

Table 1
Water quality parameters analyzed. The “Station type” can be “auto” (automatic station) or “sampling” (field campaigns). The frequency of the measurements is given in “days” and is the average calculated for all the stations for each parameter.

Parameter	# stations	Station type	# observations	Period	Frequency* (days)
• General					
Temperature (°C)	91	Auto	3,834,154	[2000, 2022]	0.06
Transparency (m)	379	Sampling	10,879	[1990, 2023]	136.01
Turbidity (NTU)	91	Auto	2,928,205	[2001, 2022]	0.08
pH – Field	92	Auto	492,565	[2001, 2022]	0.41
Conductivity (μS/cm)	92	Auto	2,893,297	[2000, 2019]	0.08
Average conductivity (μS/cm) (6 h)	91	Auto	458,691	[2001, 2019]	0.51
Total suspended solids (mg/L)	2201	Sampling	104,144	[1990, 2023]	223.84
Potassium (K) (mg/L)	156	Sampling	1618	[1990, 2023]	158.79
Sulphate (SO_4) (mg/L)	697	Sampling	22,540	[1990, 2023]	131.26
• Oxygen					
Dissolved oxygen (mg/L O_2)	91	Auto	3,309,543	[2000, 2022]	0.07
BOD5 (mg/L O_2)	2009	Sampling	102,569	[1990, 2023]	215.97
• Bacteria					
Cyanobacteria (cells/mL)	165	Sampling	3311	[1995, 2023]	121.44
• Nutrients					
Total nitrogen (TN) (mg/L N)	1803	Sampling	36,039	[2002, 2023]	279.98
Nitrate (mg/L NO_3)	2038	Sampling	95,082	[1990, 2023]	245.58
Ammonium nitrate (NH_4) (mg/L N)	236	Sampling	2835	[2003, 2019]	76.86
Total phosphorus (mg/L P)	1984	Sampling	81,438	[1990, 2023]	243.56
Phosphate (mg/L P_2O_5)	1059	Sampling	70,168	[1990, 2023]	79.27
•Carbon (C)					
Total organic C (TOC) (mg/L C)	1589	Sampling	23,901	[1998, 2023]	289.71
Dissolved organic C (DOC) (mg/L C)	480	Sampling	2779	[2011, 2023]	222.82

* Mean frequency of measurement (days).

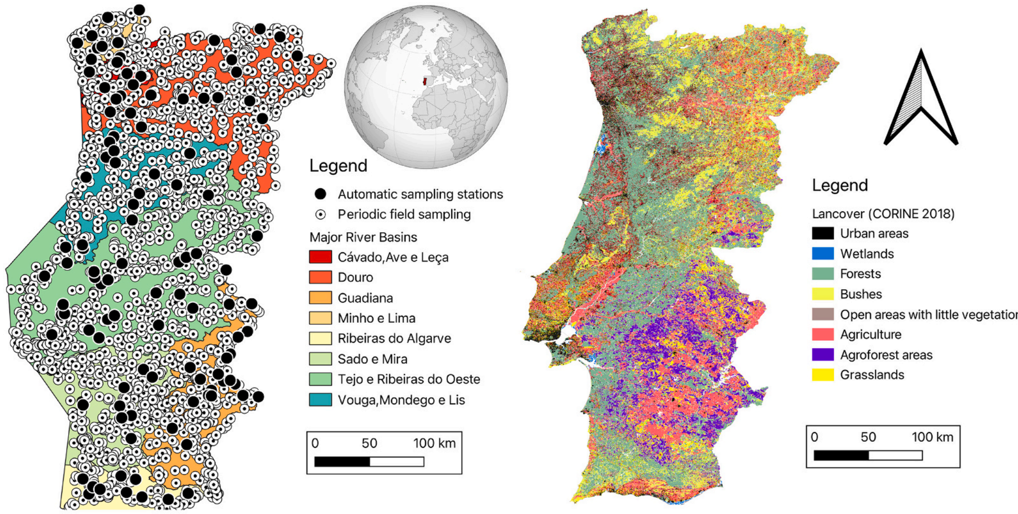

(a) Stations and basins (b) LULC 2018

Fig. 1. (a) Major river basins, automatic sampling stations (black dots; a total of 116 stations) and location of periodic sampling (white dots; a total of 3710 locations); and (b) LULC in Portugal based on CORINE 2018. More details about the characteristics of this dataset are provided in Table 1.

(12 months) and for all 3441 drainage basins, resulting in 78,4548 combinations. This analysis aimed to detect potential temporal dependencies within the dataset. Given the large number of combinations, histograms were plotted to summarize the autocorrelation structure and provide a comprehensive overview.

2.2.2. *Is LULC a strong predictor of water quality in Mediterranean basins?*

Drainage basins for all 3441 monitoring stations were delineated to evaluate land use and land cover (LULC) effects. Traditional DTM-based delineation methods, though effective, were computationally infeasible at this scale. Instead, a hybrid vector—raster approach was adopted, based on algorithms from Heberger (2023), and using MERIT–Hydro and MERIT–Basins datasets (Yamazaki et al., 2019). Despite known limitations in complex terrain, this method proved reliable when benchmarked against well-known basins.

For each delineated basin, the percentage of area covered by each LULC class was computed using the CORINE dataset (Feranec, 2016). This process was fully automated to manage the large number of basin–land cover intersections. Fig. 2 presents sample stations, their drainage basins, and associated LULC overlays. All code and algorithms used are available in the ZENODO repository.

This procedure yielded three core variables for each of the 3441

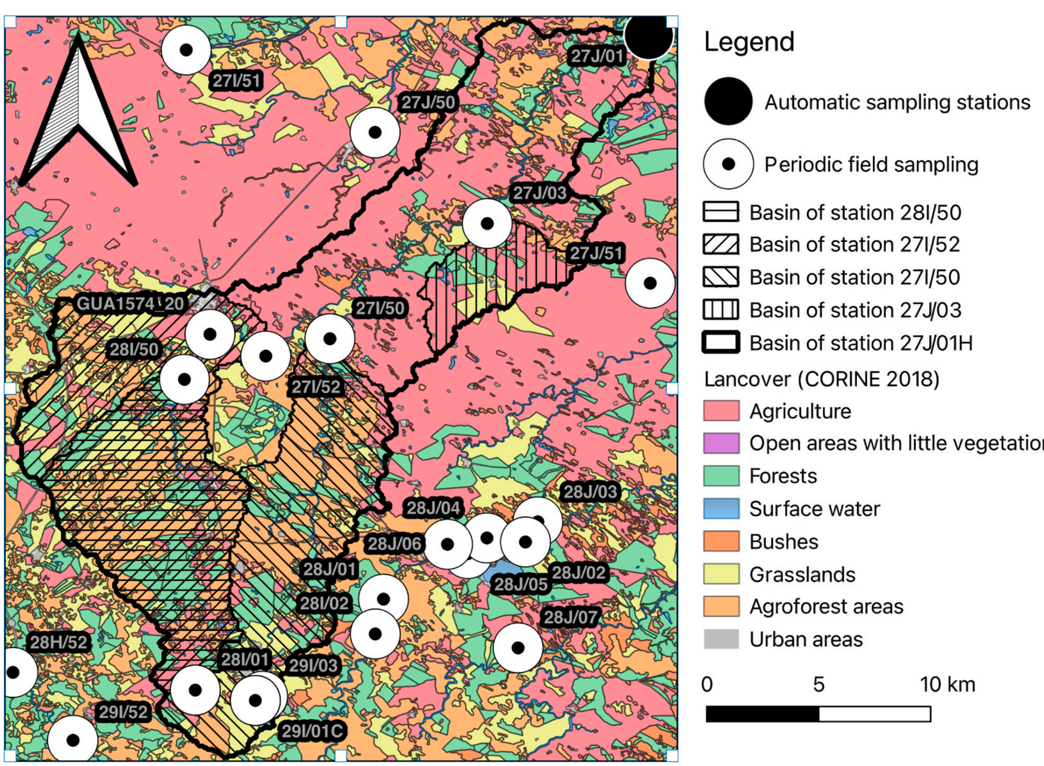

Fig. 2. LULC analyses involved delineating the drainage basins of all the 3441 stations or sampling locations involved in the study and determining the respective percentages of the different types of LULC obtained based on CORINE 2018.

station-specific drainage basins: (1) median water quality concentrations, (2) total drainage area, and (3) percentage cover of each LULC class. These were used to assess the predictive strength of LULC on water quality across Mediterranean basins using two correlation metrics: (1) Pearson's correlation coefficient (PCC, Eq. (1)) for linear relationships, and (2) Spearman's rank correlation coefficient (SRC, Eq. (2)) for monotonic trends, independent of linearity.

$$\rho_{x,y} = \frac{cov(x,y)}{\sigma_x \sigma_y} \tag{1}$$

where ρ is the Pearson correlation coefficient, x is LULC percentage (e.g., agriculture, forest), y is the median concentration of the water quality parameter, $cov(x,y)$ is the covariance between x and y, and σ_x, σ_y are their standard deviations.

$$\rho = 1 - \frac{6\sum d_i^2}{n(n^2-1)} \tag{2}$$

where ρ is Spearman's rank correlation coefficient, d_i is the difference in ranks for each observation, and n is the total number of observations.

While commonly used, these correlation metrics are particularly well-suited for this study due to its broad spatial coverage (15 national and international basins), long temporal span (34 years), geographic focus (Mediterranean), and emphasis on water quality – a dimension often overlooked relative to water quantity. This study focuses primarily on pattern identification and the correlation between LULC and water quality; yet, a preliminary application of a Generalized Additive Model (GAM) is presented in Appendix A to illustrate potential non-linear relationships that may warrant further investigation.

3. Results

3.1. Multi-basin patterns along the climate gradient

Fig. 3 shows the median values of temperature, conductivity, pH, transparency, dissolved oxygen (DO), and total suspended solids (TSS) calculated for all stations covering all basins. Across the basins, the median water temperature increases southwards (Fig. 3a) and boxplot

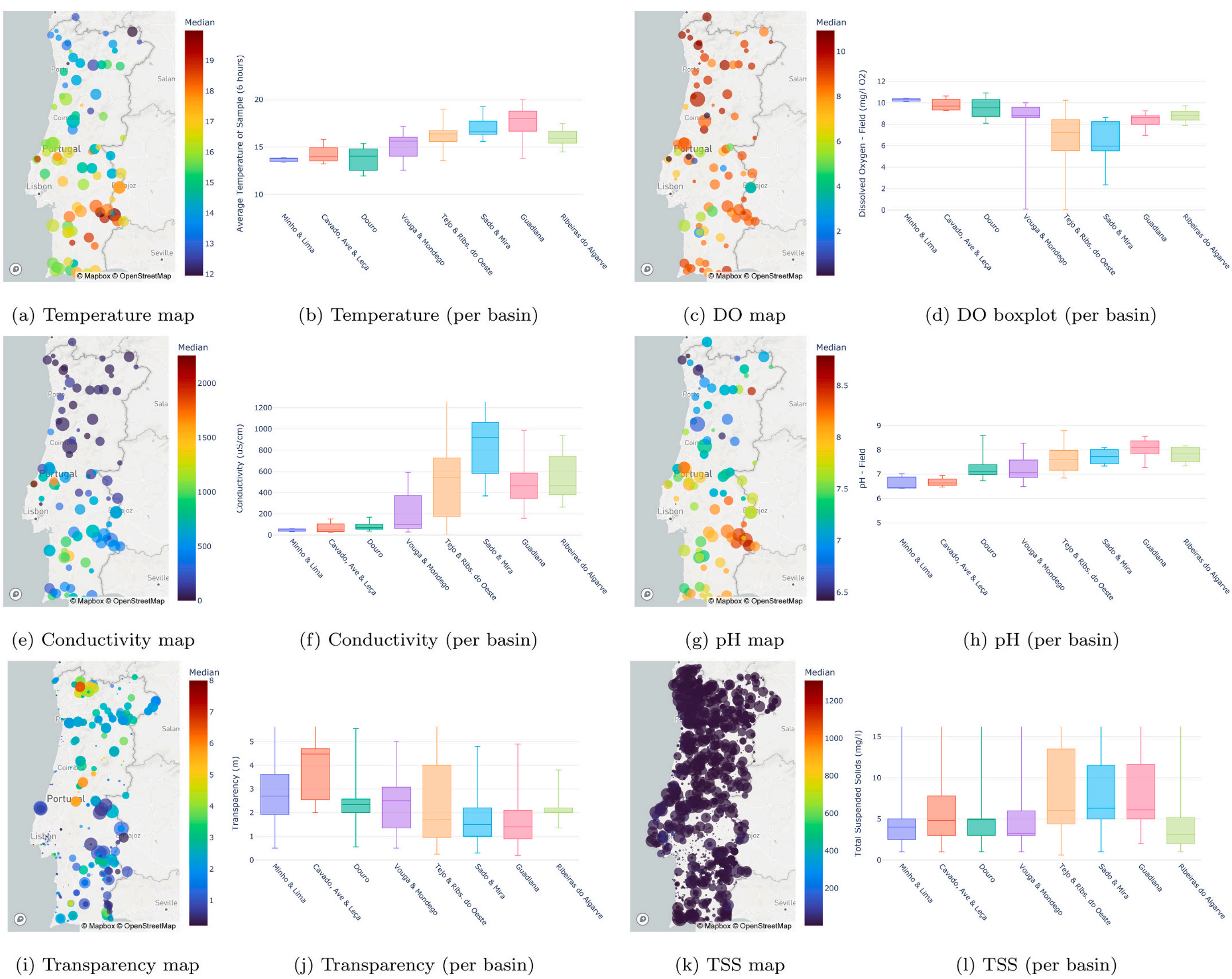

(a) Temperature map (b) Temperature (per basin) (c) DO map (d) DO boxplot (per basin)

(e) Conductivity map (f) Conductivity (per basin) (g) pH map (h) pH (per basin)

(i) Transparency map (j) Transparency (per basin) (k) TSS map (l) TSS (per basin)

Fig. 3. Median temperature, conductivity, pH, transparency, dissolved oxygen (DO), and total suspended solids (TSS) across stations, including spatial distributions maps and box plots of median concentrations per river basin. In the boxplots, the x-axis corresponds to the 8 river basin groups, which are ordered from north to south. Each map in the figure shows the spatial distribution of an individual parameter and is accompanied by an adjacent boxplot showing the medians concentrations grouped by major river basins and ordered along the north (cooler, rainier) to south (warmer, dried) climate gradient (left to right in the x-axis). In the maps, the circles display (1) different colours to indicate the median parameter value (e.g., concentration) and (2) different sizes to indicates the relative dimension of the dataset used to generate the medians.

(Fig. 3b). Parameters like conductivity, pH, and TSS follow a similar spatial north-to-south distribution. Conversely, DO and transparency decrease as the basin's location moves southwards. While for DO, the change is likely related to the inverse relationship between temperature and oxygen saturation concentrations, the transparency patterns can be caused by several factors that include (a) more precipitation in northern basins leading to increased streamflow thus higher dilution capacity, (b) increased temperatures and light period in southern basins leading to eutrophication and algae blooms (this also amplifying further DO depletion due to increased microbial respiration), and (c) less vegetation in southern basin due to dried conditions leading to increased erosion.

Fig. 4 shows the results of various nutrient and carbon species and groups, namely TN, NO_3, TP, P_2O_5, TOC and SO_4. Results show that TN, TOC, and SO_4 increase southwards, except for the southernmost basins (Ribeiras do Algarve, last bar in each box plot), which have the smallest drainage basins and, therefore, likely provide less opportunity for runoff mobilization of soil constituents from agricultural lands. TN and TOC include dissolved and particulate forms; thus, an increase in concentrations from north to south (as precipitation decreases and temperatures increase) may be related to a reduced streamflow dilution capacity (increasing concentrations), as well as an increase in agricultural land (see Fig. 1).

Conversely, NO_3 and P_2O_5 concentrations seem to follow the opposite pattern, generally decreasing southwards as precipitation also decreases. In this case, this may be partially related to a decrease in precipitation, reducing the runoff transport capacity of soluble nutrients. Also, although maybe of limited effect, is that since NO_3 and P_2O_5 are both biogenically produced through oxidation processes, a decrease in oxygen levels southwards (see Fig. 3c and d) could potentially limit nitrification (for N) and mineralization (for P) rates. The patterns of TP are less clear but seem to show an increase towards the central part of Portugal followed by a decrease as basins move southwards.

3.2. Differences in seasonal effects across regions

Fig. 5 shows the seasonal medians per basin for DO, transparency, cyanobacteria, TOC, TN, NO_3, TP, and PO_4. As expected, DO levels are higher during the wet season for all large and small basins. Transparency

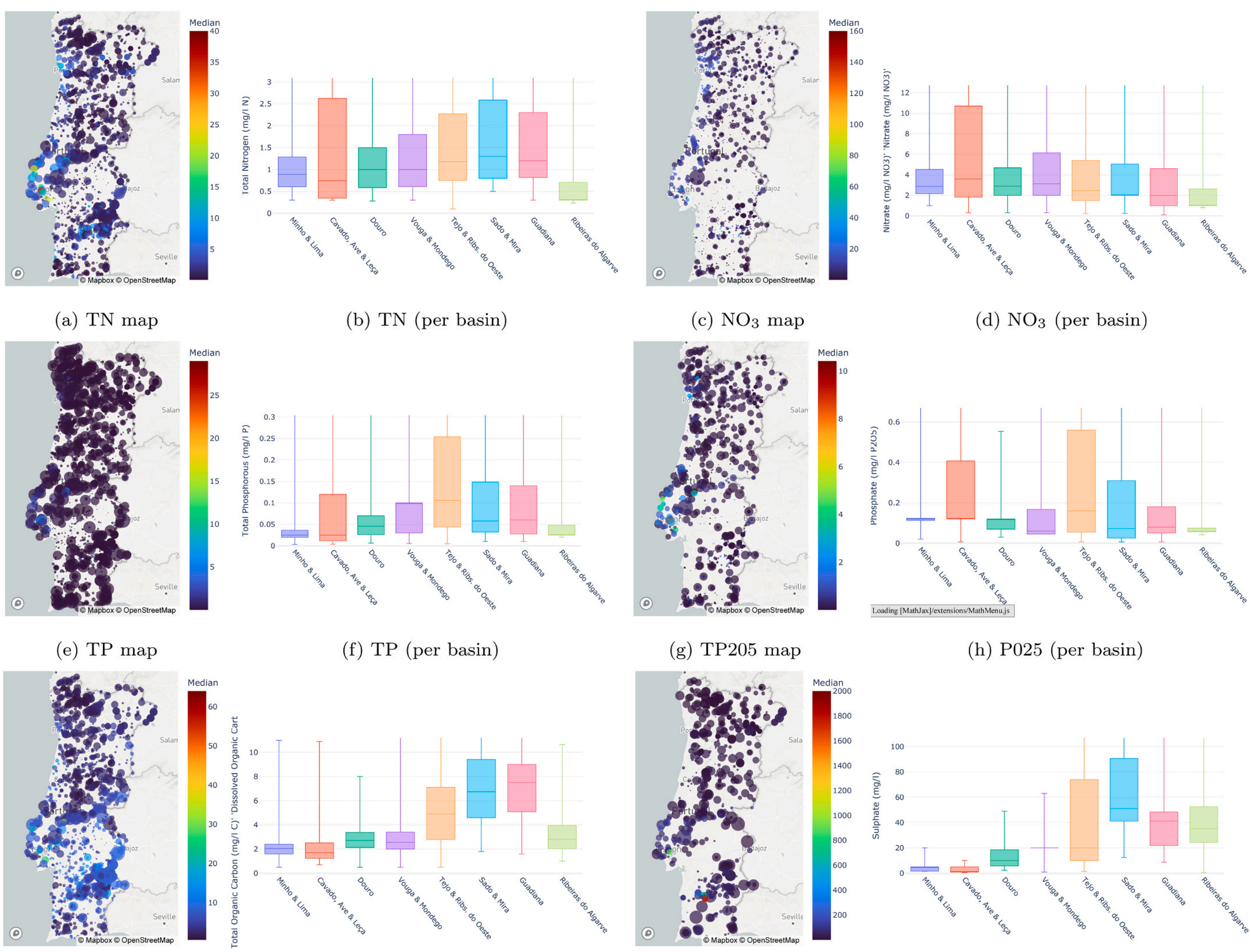

(a) TN map (b) TN (per basin) (c) NO_3 map (d) NO_3 (per basin)

(e) TP map (f) TP (per basin) (g) TP205 map (h) P025 (per basin)

(i) TOC map (j) TOC (per basin) (k) SO_4 map (l) SO_4 (per basin)

Fig. 4. Median values of total nitrogen (TN), nitrate (NO_3), total phosphorous (TP), phosphate (P_2O_5), total organic carbon (TOC) and sulphate (SO_4) across stations, including spatial distribution maps and box plots of median concentrations per river basin. In the boxplots, the x-axis corresponds to the 8 river basin groups, which are ordered from north to south. Each map in the figure shows the spatial distribution of an individual parameter and is accompanied by an adjacent boxplot showing the medians concentrations grouped by major river basins and ordered along the north (cooler, rainier) to south (warmer, dried) climate gradient (left to right in the x-axis). In the maps, the circles display (1) different gradients to indicate the median parameter value (e.g., concentration) and (2) different sizes to indicates the relative size of the dataset used to generate the medians.

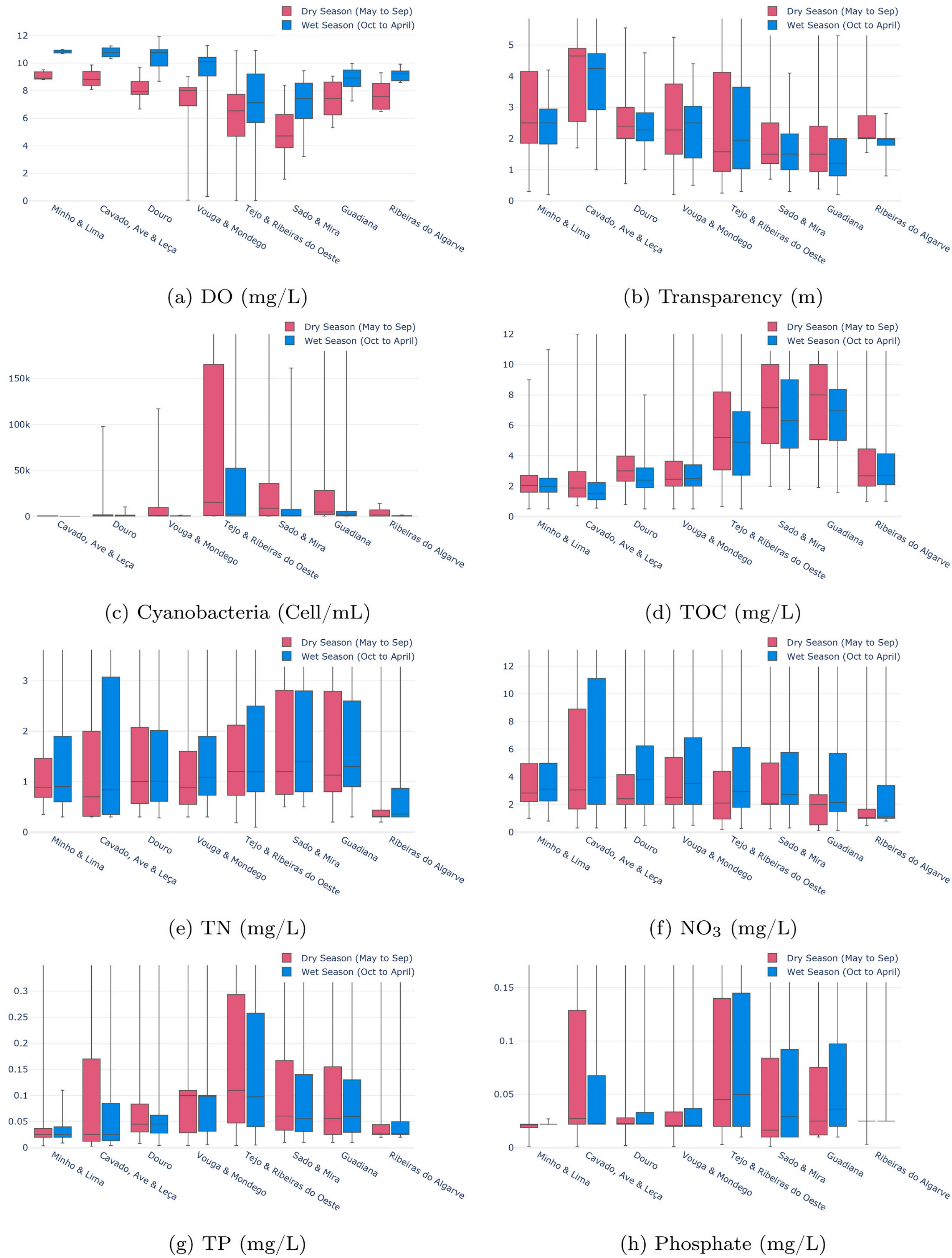

Fig. 5. Boxplots of concentrations between seasons and across stations for (a) DO, (b) transparency, (c) cyanobacteria, (d) TOC, (e) TN, (f) NO_3, (g) TP, and (h) phosphate. The x-axis corresponds to the 8 river basin groups, which are ordered from north to south.

is similar between seasons but has a wider amplitude during the dry season, likely due to periods of high algae productivity and little precipitation resulting in reduced dilution. A similar pattern is observed for cyanobacteria but in an even more pronounced manner. Also TP observes a similar trend, which in this case may be also related to dried conditions in the summer leading to reduced vegetation thus providing less protection against soil erosion (Alliaume et al., 2014; Francia Martínez et al., 2006; Gómez et al., 2009). In turn, TN and NO_3 levels seem to show the opposite pattern, depicting a higher amplitude during the wet season. This may be related to (a) intense winter rainfall-runoff events causing the rapid mobilising of N from the soil, (b) less uptake of N by plants and algae during winter (lower primary productivity), and (c) higher mineralization rates. In the case of NO_3, the increase during the wet season may also be linked to increased DO levels promoting nitrification.

3.3. *Comparing multidecadal trends & inflection points across basins*

Fig. 6 shows the evolution of DO, BOD_5, TSS, TOC, TN, NO_3, TP, and P_2O_5 over the last 3.5 decades (increments of 5 years) through boxplots generated for each basin. Results show that DO levels have been generally stable in northern basins but slightly increased in southern ones, particularly in the Sado & Mira, and Guadiana basins. For BOD_5, TSS, DOC, TP and P_2O_5, a general reduction in concentrations is observed mostly for central and southern basins, namely in Tejo & Ribeiras do Oeste, and Guadiana, which showed markedly higher concentrations than northern basins before 2005. These substantial concentration drops after 2005 are notable, suggesting an improvement in the general status of the water bodies. The shift coincides with an extreme drought that occurred in 2004/05 (Santos et al., 2007) and also the construction of the Alqueva dam in 2002 with subsequent expansion in the irrigation perimeter (52,000 ha by 2012; 68,000 ha by 2013; 120,000 ha by 2016); however, a direct causal effect cannot be established. On the other hand, NO_3 and P_2O_5 levels seem to follow the opposite trend, particularly in the southern basins. While in northern-central basins, from Minho & Lima to Tejo & Ribeiras do Oeste, a substantial drop in NO_3 and P_2O_5 concentrations is observed starting in 2010 (lasting to the present day), the southern basins (particularly Sado & Mira, and Guadiana) show the opposite trend with an increase in concentrations, which may be related to the steady increase of irrigated agriculture, with the use of higher amounts of production factors as fertilisers and pesticides, after the Alqueva reservoir construction in 2002, and introduced newly irrigated areas that total 130,000 ha in 2024 (with planned to continue growing).

3.4. *Is LULC a predictor of water quality in these Mediterranean basins?*

Fig. 7 shows the "Pearson Correlation Coefficient (PCC)" and "Spearman Rank Coefficient (SRC)" relating the various water quality parameters with the percentage of LULC of the corresponding drainage basins. Results show a consistent positive correlation between most water quality parameter concentrations and the fraction of agricultural land [PCC = [0.1, 0.53]; SRC = [0.17, 0.56]] and grassland [PCC = [0.05, 0.46]; SRC = [0.07, 0.35]] areas in the respective drainage basin. Exception goes for two parameters, DO and transparency, which show a negative correlation [PCC(DO) = −0.35; PCC(transparency) = −0.38; SRC(DO) = −0.39; SRC(transparency) = −0.40], reinforcing the general water quality decline tendency as agriculture expands in the basins. As basin size increases, values of water quality parameters seem to show a slight tendency to decrease as well, suggesting dilution and retention effects [PCC = [−0.1, −0.0]]. Also, as the fraction of forests, open areas with little vegetation (likely unfertilised), and bushes increase, an improvement in the water quality status is observed, with reduced nutrient concentrations [PCC = [−0.5, −0.07]; SRC = [−0.51, −0.1]] and increased DO [PCC = 0.23; SRC = 0.3) and transparency levels [PCC = 0.09; SRC = 0.09). Forests are well known to act as a buffer against contamination, helping maintain and improve water quality in streams and decreasing soil erosion (Zhou et al., 2017).

Finally, as the proportion of surface water areas (e.g., lakes, reservoirs, estuaries, and wetlands) increases within a drainage basin, concentrations of certain constituents (e.g., pH, SO_4, DOC, TOC, TP, and K) generally rise, while most others (e.g., turbidity, cyanobacteria, and phosphate (PO_4)) tend to decrease. For pH, the increase [PCC = 0.16; SRC = 0.18] may be explained by the general positive relationship between surface water area and water deep in lakes and ponds, which are more susceptible to stratification, causing a higher pH. For DOC and TOC, the positive relationship with water surface area [PCC(DOC) = 0.09; SRC(DOC) = 0.31; PCC(TOC) = 0.14; SRC(TOC) = 0.32] may be explained by increased biomass in larger lakes and ponds, while the negative relationship with P_2O_5 [PCC = −0.1; SRC = −0.19] is probably related to increased sorption to sediments that tends to increase with high pH. Phosphorous can remain adsorbed to sediments for a long period of time, and when anoxic conditions occur (during dry periods), it can be resuspended. As for BOD_5, the decrease [PCC = −0.1; SRC = −0.03] is probably related to technology improvement and resizing of sewage treatment plants, contributing to organic pollution reduction in freshwaters.

4. Discussion

4.1. *Dominant cross-basin water quality trends and natural-human drivers*

Understanding how (and why) key natural and antropogenic conditions change the overall water quality status across different Mediterranean river basins is critical to identify common and diverging patterns and drivers across regions. Table 2 explores the findings of the previous sections towards answering these questions. The table brings together climate (precipitation and temperature) and main LULC-types information to help interpret the key water quality patterns.

The table shows that the number of problematic water quality parameters tends to increase southwards, except for the "Ribeiras do Algarve" that comprises a group of small creeks with small drainage basins (probably leading to lower runoff pollution mobilization capacity). This latitude-driver water quality deterioration is inversely related to precipitation/temperature patterns that decrease/increase southwards, hinting at concentration increases being driven by lower natural dilution and buffering capacity. Results show that NO_3 remains the most pervasive problem across most of the Mediterranean basins examined, although in recent years concentrations have declined in certain basins (e.g., Cavado, Ave & Leça, and Ribeiras do Algarve). Conversely, the Guadiana and Sado & Mira river basins have experienced increased NO_3 concentrations, likely due to the combined effects of agricultural expansion, fertilizer use, and limited precipitation, which reduces dilution of pollutants. Notably, these basins have among the highest percentages of agricultural land and lowest forest coverages, which combined with low precipitation rates, result in them exhibiting the largest range of problematic water quality parameters, including TSS, BOD, NO_3, TP, and DOC.

The Douro River basin represents an interesting exception. Despite having one of the highest proportions of agricultural land (30 % of the total area), concentrations of most pollutants have been declining; yet, with NO_3 remaining as the primary parameter of concern. The considerable annual precipitation in this basin is likely a key factor in attenuating the water quality problems through dilution. Additionally, the predominance of traditional agriculture in the northern basins, as opposed to the intensive, irrigated agriculture more typical in the south, may also help justify the relatively lower impact of agriculture on water quality in this region.

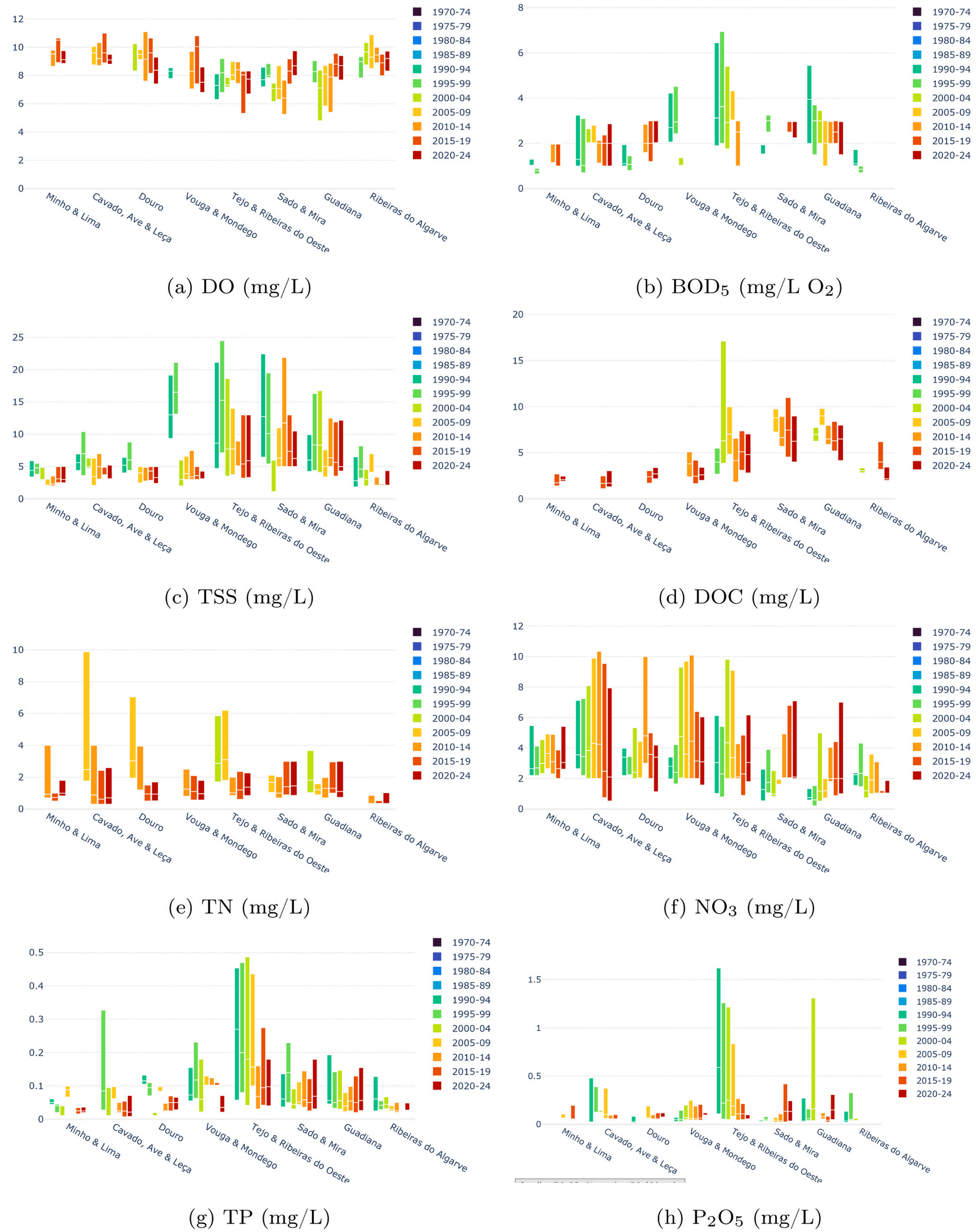

(a) DO (mg/L) (b) BOD_5 (mg/L O_2)
(c) TSS (mg/L) (d) DOC (mg/L)
(e) TN (mg/L) (f) NO_3 (mg/L)
(g) TP (mg/L) (h) P_2O_5 (mg/L)

Fig. 6. Boxplots of concentrations from 1970 to 2024. The x-axis corresponds to the 8 river basin groups, which are ordered from north to south.

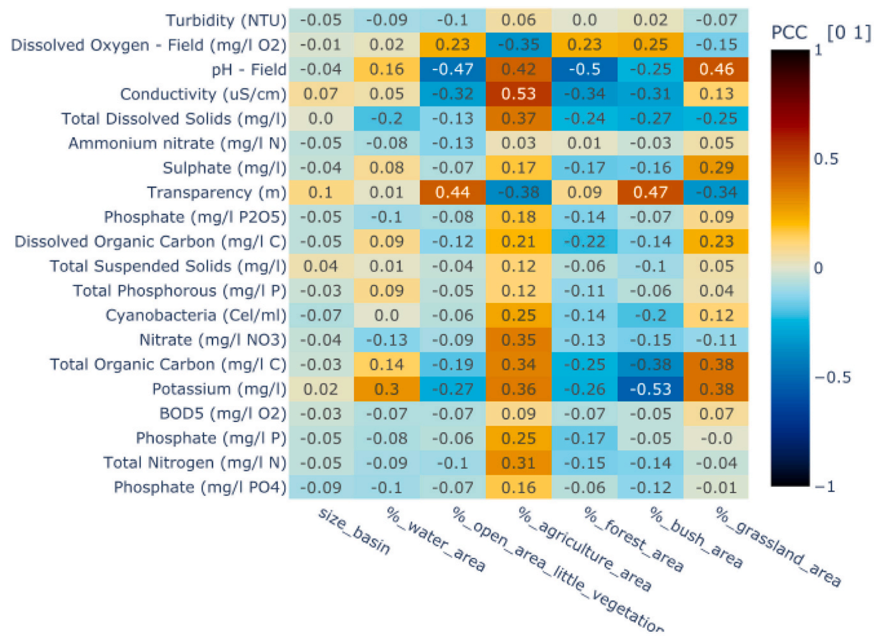

(a) PCC

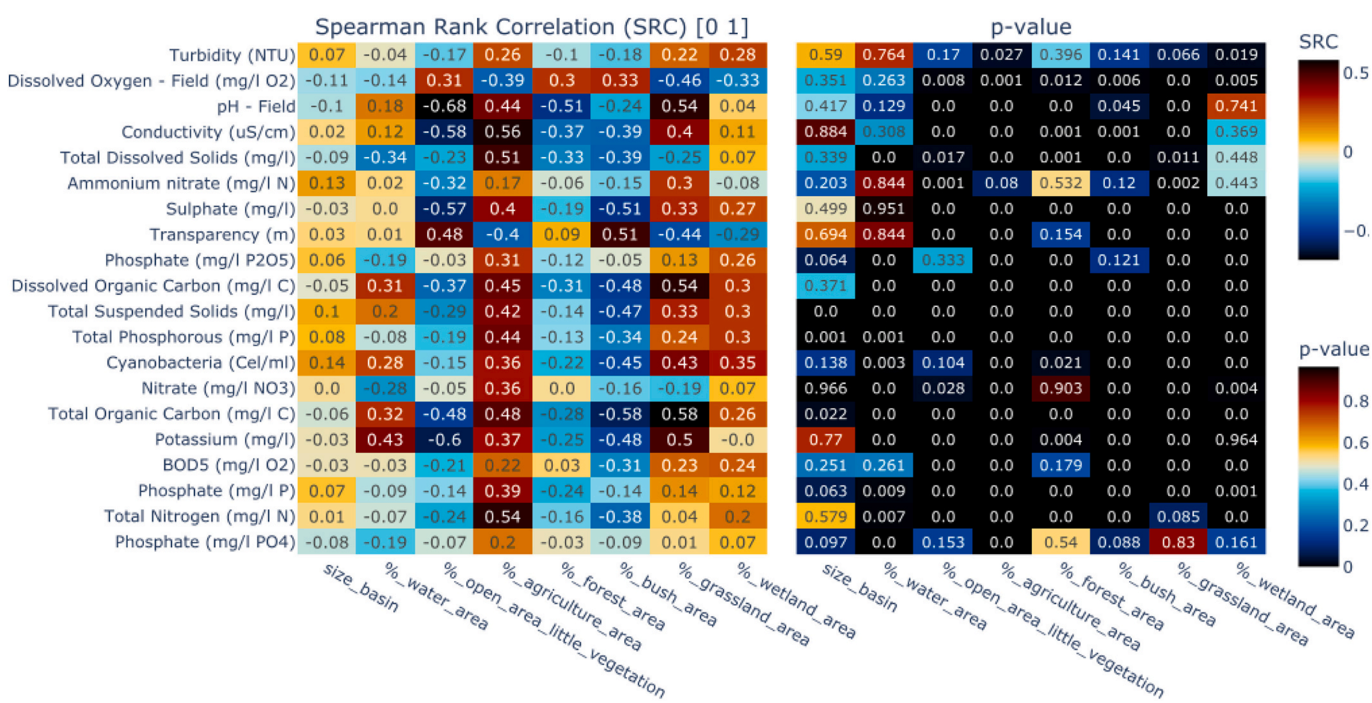

(b) SRC

Fig. 7. Correlation coefficients: (a) Pearson correlation coefficient (PCC) and (b) Spearman rank coefficient (SRC).

4.2. *Effects of climate change*

Disentangling the effect of climate change on water quality patterns is not trivial due to the combination and superposition of natural and antropogenic effects. To help with this, 5-year average annual precipitation and air temperature trends have been obtained from the Portuguese Institute for Sea and Atmosphere (IMPA) for the period of 1930 and 2021 (Fig. 8) to help discuss the historical water quality trends observed in Section 4.1. Annual precipitation has been decreasing over the last decades, while air temperature follows the global trend of steady increase. The two years with the most pronounced variability in water quality were 2005 and 2010, generally coinciding with the occurrence of major droughts (2004/05 and 2013/14).

In 2005, a drop in BOD_5, TSS, DOC, TP and P_2O_5 was observed particularly in the southern basins. Around this year, the most pronounced climatic change observed was a decrease in precipitation that started in 2004 and remained abnormally low thereafter. A precipitation decrease generally leads to runoff reduction and, consequently, a decrease in erosion, and mobilization of diffuse pollution, one of the main factors contributing to the increase in surface water concentrations of the aforementioned parameters.

In 2010, NO_3 and P_2O_5 decreased in the northern basins and

Table 2
Summary of key water quality parameter changes and problems for each basin.

Basin	Mean annual precipitation[a] & air temp.[b]	Main LULC[c] (%)	Main parameters trends (1970–2024)		Problematic parameters (last 5 years)
			Increase	Decrease	
Minho & Lima	1900 mm 14 °C	37 % forests 28 % shrub area 16 % agriculture	NO_3	TSS	–
Cavado, Ave & Leça	1923 mm 14.5 °C	36 % forests 21 % agriculture 18 % shrub area	BOD_5	TSS, TN, NO_3, TP, P_2O_5	NO_3
Douro	984 mm 14.5 °C	35 % forests 30 % agriculture 25 % shrub area	BOD_5	DO, TN, TP	NO_3
Vouga & Mondego	1064 mm 15.5 °C	55 % forests 20 % agriculture 13 % shrub area	NO_3	TSS, DOC, TN, P_2O_5	NO_3
Tejo & Rib. do Oeste	791 mm 16 °C	42 % forests 24 % agriculture 10 % agroforestry	DO, DOC	BOD_5, TSS, TN, TP, P_2O_5	DO, BOD_5, TSS, DOC, NO_3, TP
Sado & Mira	592 mm 17 °C	36 % forests 24 % agriculture 19 % agroforestry	DO, NO_3, P_2O_5	TSS, DOC	DO, TSS, DOC, NO_3, TP, P_2O_5
Guadiana	367 mm mm 18 °C	31 % agriculture 23 % forests 22 % agroforestry	DO, NO_3	BOD_5, DOC	DO, BOD_5, TSS, DOC, TN, NO_3, TP
Rib. do Algarve	423 mm 18 °C	36 % forests 26 % shrub area 24 % agriculture	DO	TSS, NO_3, TP	–

[a] Between 1971 and 2000 (mm) obtain from IPMA's Portal do Clima.
[b] Average calculated based on www.weather-atlas.com.
[c] Determined based on CORINE 2018.

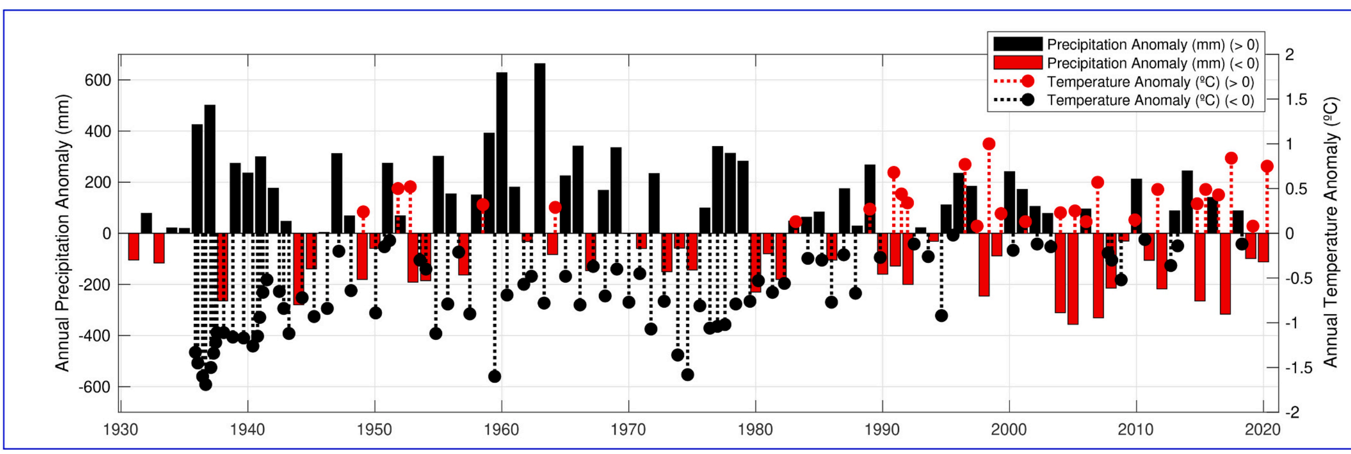

Fig. 8. Precipitation and air temperature anomalies between 1981 and 2010 (upper and lower panels respectively). Data obtained from IPMA (Instituto Português do Mar e da Atmosfera, Portuguese Institute for the Ocean and Atmosphere). The data series was obtained based on about 50 stations.

increased in the southern ones. To help investigate the causes for these regional differences, Fig. 9 shows the mean annual rainfall anomalies have been obtained from Portela et al. (2020) for the period of 1913 and 2019. The figure highlights a more pronounced decrease in rainfall in the northern parts of Portugal, which can help explain the NO_3 and P_2O_5 decrease in the northern basin, as less precipitation leads to less runoff nutrient mobilization. In turn, the less pronounced decrease in precipitation in the south suggests that the associated reduction in runoff nutrient mobilization, which is weaker in the south, is overridden by the intensification of agricultural activities in the south, particularly after the building of the Alqueva dam in 2002 (52,000 ha of new irrigated area by 2012, increasing to 68,000 ha by 2013, and to 120,000 ha by 2016).

4.3. Limitations and future work

Some limitations of this study are noted. First, groundwater data was not included, as the study's primary focus was on surface water quality. Although this exclusion was intentional, future analyses that incorporate groundwater data may uncover important interactions between surface and groundwater that could help explain some of the water quality patterns observed. Another limitation is the lack of synchronous hydrological and water quality data, which could have provided insights into, for example, discharge-water quality relationships. Due to the hydrological stations being located in different areas and not synchronized with water quality stations, establishing these relationships was not feasible. Instead, precipitation was used as a proxy for runoff and streamflow. Future studies should aim to establish more direct connections between water quality and streamflow across these, and other, Mediterranean basins. Finally, data on natural and management-related

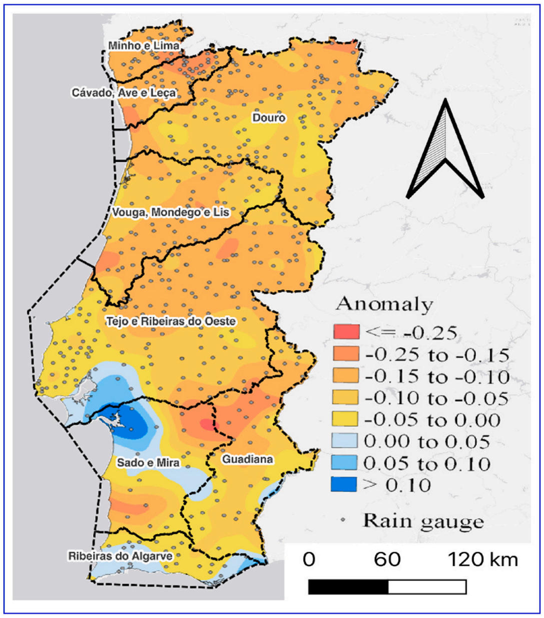

Fig. 9. Mean annual rainfall anomalies.
(Adapted from Portela et al. (2020).)

drivers from upstream basin areas located in Spain was limited. Future research should seek collaboration with Spanish researchers for integration of new datasets and expand the research further.

5. Conclusions

A 3-decade long water quality dataset (1990 to 2014) covering a 89,015 km^2 Mediterranean region and 15 major national and international river basins, located along a climate gradient, has been examined to help disentangle the key natural and anthropogenic drivers of water quality in Mediterranean regions. The analyses is not trivial because the effects are compounded by (1) a climate gradient, (2) climate variability, (3) LULC diversity, and (4) climate change.

The data showed a strong north-to-south variability in most water quality parameters (cooler-wetter north Vs hotter-drier south). DO and transparency decrease southwards, while TN, TOC, and SO_4 increase, driven by more intensive agriculture and reduced precipitation, which weakens stream dilution. DO and transparency levels are higher during the wet season across basins. In contrast, TN and NO_3 levels are more variable in the wet season due to nutrient mobilization from intense rainfall-runoff. From 1990 to 2014, DO remained fairly stable, but BOD, TSS, DOC, and TP declined, whereas NO_3 and P_2O_5 rose, particularly after 2005. Reduced BOD_5 and TP may relate to improved sewage treatment, while the increase in NO_3 and P_2O_5 likely stems from intensified agriculture and fertilizer use. Indeed, agriculture and grassland expansion correlated positively with most parameters, except DO and transparency, indicating a negative impact and general degradation effect.

Large-scale water quality studies that offer integrated, comparative analyses of river basins are scarce not only in Mediterranean regions but across Europe and worldwide. This study seeks to bridge that gap, providing insights valuable for decision-making, process understanding, and large-scale modeling. We think that this contribution will be useful not only to academia, but also regional and national authorities, which will have now more information to allow them to prioritize water quality problems to solve and resources to mobilize (where, when and how).

CRediT authorship contribution statement

Diogo Costa: Writing – review & editing, Writing – original draft, Visualization, Validation, Supervision, Software, Resources, Project administration, Methodology, Investigation, Funding acquisition, Formal analysis, Data curation, Conceptualization. **Jian Liu:** Writing – review & editing, Validation, Methodology, Conceptualization. **Patricia Palma:** Writing – review & editing, Validation, Methodology, Conceptualization.

Declaration of competing interest

The authors declare the following financial interests/personal relationships which may be considered as potential competing interests: Diogo Costa reports financial support was provided by University of Évora. Diogo Costa reports financial support was provided by Mediterranean Institute for Agriculture Environment and Development. Diogo Costa reports institutional support was provided by Center for Sci-Tech Research in Earth System and Energy. Jian Liu reports financial support was provided by Norwegian Institute of Bioeconomy Research. Patricia Palma reports financial support was provided by Polytechnic Institute of Beja. Diogo Costa reports financial support was provided by Institute for Global Change and Sustainability. If there are other authors, they declare that they have no known competing financial interests or personal relationships that could have appeared to influence the work reported in this paper.

Acknowledgements

This work is funded by National Funds through FCT – Foundation for Science and Technology under the Projects UIDB/05183 and Water4All/003/2023 It was supported by the research centers MED (Instituto Mediterrâneo para a Agricultura, Ambiente e Desenvolvimento, Mediterranean Institute for Agriculture, Environment and Development) and CREATE (Centre for Sci-Tech Research in Earth Systems and Energy) at the University of Évora. The authors would like to acknowledge also the support of CHANGE (Instituto para as Alterações Globais e Sustentabilidade, Global Change & Sustainability Institute).

Appendix A. Autocorrelation analysis

Fig. A.1 presents the cumulative distributions of autocorrelation coefficients computed across all parameter, station, and lag combinations. The results indicate that while some degree of autocorrelation is present, it is limited to a relatively small subset of parameter-station pairs and is primarily confined to short lags (1-month and 2-month). This is a limited persistence that does not compromise the robustness of the broader analysis. The presence of autocorrelation in certain cases is expected, particularly for parameters influenced by seasonal or climatic variability—such as dissolved oxygen and water temperature—which are known to respond to fluctuations in air temperature.

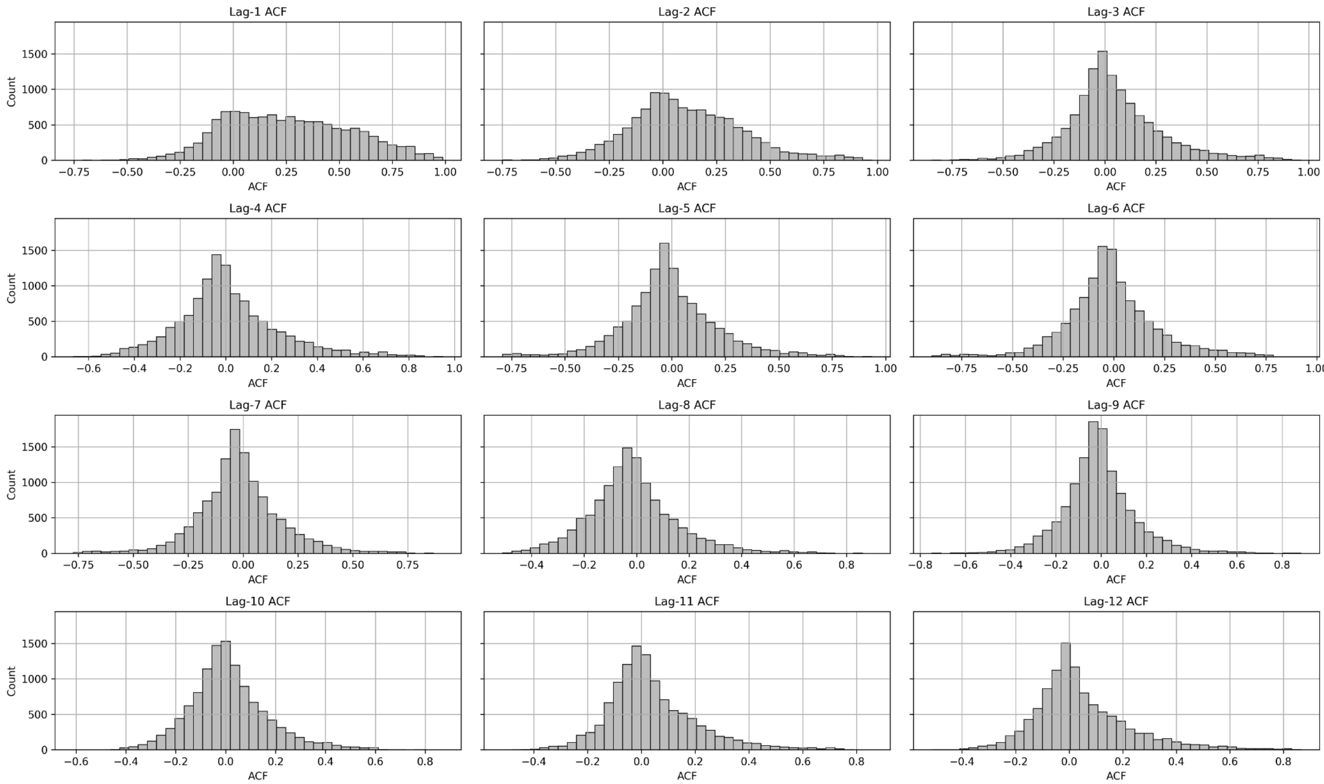

Fig. A.1. Autocorrelation coefficients for all 19 water quality parameters, 3441 stations, considering 1–12 month lags.

Appendix B. Generalized Additive Model (GAM) - preliminary analysis

To investigate potential non-linear relationships between land use and land cover (LULC) proportions and median water quality concentrations, Generalized Additive Models (GAMs) were employed. This preliminary analysis is intended to inform and guide subsequent research efforts. GAMs generalize linear models by incorporating smooth, data-driven functions of predictor variables, enabling the modeling of complex, non-parametric relationships without assuming a specific functional form. In this study, separate GAMs were fitted for each water quality parameter using the percentage of individual LULC classes as predictors, across 3441 station-specific drainage basins. This approach facilitates the identification of threshold responses and non-linear trends that may not be captured by conventional correlation metrics. The general structure of the models applied in this study is as follows:

$$Y = \alpha + f_1(X_1) + f_2(X_2) + \cdots + f_p(X_p) + \varepsilon \quad \text{(B.1)}$$

where Y is the median water quality concentration, X_i represents the percentage of a given LULC class, f_i are smooth functions estimated from the data, α is the intercept, and ε is the error term.

Fig. B.1 shows the fitted GAMs for selected parameters relating them particularly with percentage area of the respective drainage basins occupied by (a) agriculture and (b) forest. All remaining results are available in the ZENODO database.

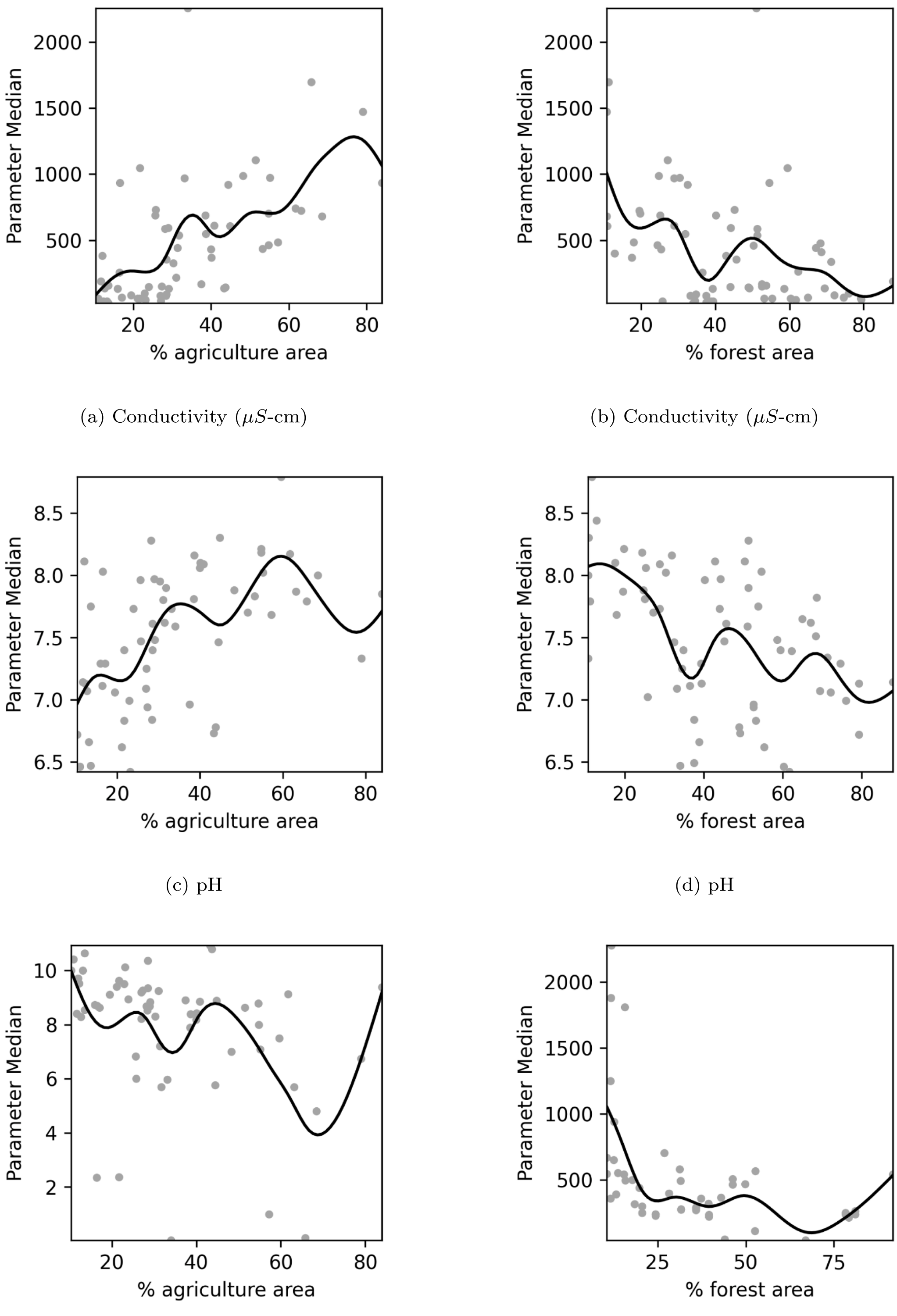

(a) Conductivity (μS-cm)

(b) Conductivity (μS-cm)

(c) pH

(d) pH

(e) Dissolved Oxygen (mg/L O_2)

(f) Total Dissolved Solids (mg/L)

Fig. B.1. Smooth functions estimated through GAMs relating selected water quality parameters with (a) % agriculture and (b) % forest cover.

Table B.1 summarizes the GAM performance for the selected parameters of Fig. B.1.

Table B.1
Summary of GAM performance for the selected parameters of Fig. B.1.

Parameter	Percentage area	R-squared	p-Value	EDF
Conductivity (μS-cm)	Agriculture	0.41	>0.001	8.68
Conductivity (μS-cm)	Forest	0.31	>0.001	9.18
pH	Agriculture	0.4	>0.001	8.73
pH	Forest	0.4	>0.001	9.18
Dissolved oxygen (mg/l)	Agriculture	0.3	>0.001	8.70
Total dissolved solids (mg/l)	Forest	0.4	>0.001	8.06

The Generalized Additive Models (GAMs) indicate statistically significant ($p < 0.001$) and non–linear relationships between water quality parameters and land use types, with moderate explanatory power (R^2 ranging from 0.3 to 0.41). Conductivity and pH showed the strongest associations with both agricultural and forested land covers, while dissolved oxygen and total dissolved solids were more weakly explained. The effective degrees of freedom (EDF ≈ 8–9) suggest complex, smooth relationships, reinforcing the importance of accounting for non–linearity in land use–water quality interactions.

Data availability

Data and code developed for this research can be downloaded from ZENODO and GitHub repositories.

References

Alliaume, F., Rossing, W., Tittonell, P., Jorge, G., Dogliotti, S., 2014. Reduced tillage and cover crops improve water capture and reduce erosion of fine textured soils in raised bed tomato systems. Agric. Ecosyst. Environ. 183, 127–137. https://doi.org/10.1016/j.agee.2013.11.001.

Almeida, P., Albuquerque, T., Antunes, M., Ferreira, A., Pelletier, G., 2021. Effects of wastewater treatment plant's discharges on a freshwater ecosystem—a case study on the Ramalhoso River (Portugal). Water Air Soil Pollut. 232, 206.

Alves-Ferreira, J., Vara, M.G., Catarino, A., Martins, I., Mourinha, C., Fabião, M., Costa, M.J., Barbieri, M.V., de Alda, M.L., Palma, P., 2024. Pesticide water variability and prioritization: the first steps towards improving water management strategies in irrigation hydro-agriculture areas. Sci. Total Environ. 917, 170304. https://doi.org/10.1016/j.scitotenv.2024.170304.

Azevedo, I.C., Duarte, P.M., Bordalo, A.A., 2008. Understanding spatial and temporal dynamics of key environmental characteristics in a mesotidal Atlantic estuary (Douro, NW Portugal). Estuar. Coast. Shelf Sci. 76, 620–633. https://doi.org/10.1016/j.ecss.2007.07.034 submarine groundwater discharge studies along the Ubatuba coastal area in south-eastern Brazil.

Bellém, Fernando, N., S., Morais, M., 2013. Cyanobacteria toxicity: potential public health impact in South Portugal populations. J. Toxicol. Environ. Health A 76, 263–271. https://doi.org/10.1080/15287394.2013.757204.

Bennett, J., 2010. OpenStreetMap. Packt Publishing Ltd.

Cabecinha, E., Cortes, R., Ângelo Pardal, M., Cabral, J.A., 2009. A stochastic dynamic methodology (STDM) for reservoir's water quality management: validation of a multi-scale approach in a south European basin (Douro, Portugal). Ecol. Indic. 9, 329–345. https://doi.org/10.1016/j.ecolind.2008.05.010.

Catarino, A., Martins, I., Mourinha, C., Santos, J., Tomaz, A., Anastácio, P., Palma, P., 2024. Water quality assessment of a hydro-agricultural reservoir in a Mediterranean region (case study—Lage Reservoir in southern Portugal). Water 16. https://doi.org/10.3390/w16040514.

Company, R., Serafim, A., Lopes, B., Cravo, A., Shepherd, T., Pearson, G., Bebianno, M., 2008. Using biochemical and isotope geochemistry to understand the environmental and public health implications of lead pollution in the lower Guadiana River, Iberia: a freshwater bivalve study. Sci. Total Environ. 405, 109–119. https://doi.org/10.1016/j.scitotenv.2008.07.016.

Confesor, R., Bechmann, M., Deelstra, J., Øygarden, L., 2023. Nibio Report. 2023. 9(84). https://hdl.handle.net/11250/3069581.

Costa, D., Sutter, C., Shepherd, A., Jarvie, H., Wilson, H., Elliott, J., Liu, J., Macrae, M., 2022. Impact of climate change on catchment nutrient dynamics: insights from around the world. Environ. Rev. 31, 4–25. https://doi.org/10.1139/er-2021-0109.

Cravo, A., Cardeira, S., Pereira, C., Rosa, M., Alcântara, P., Madureira, M., Rita, F., Correia, C., Rosa, A., Jacob, J., 2019. Nutrients and chlorophyll-a exchanges through an inlet of the Ria Formosa Lagoon, SW Iberia during the productive season – unravelling the role of the driving forces. J. Sea Res. 144, 133–141. https://doi.org/10.1016/j.seares.2018.12.001.

EC, 2021. Report from the European Commission to the European Parliament on the Implementation of Council Directive 91/676/EEC concerning the protection of waters against pollution caused by nitrates from agricultural sources based on member state reports for the period 2016–2019. https://eur-lex.europa.eu/legal-content/EN/TXT/PDF/?uri=CELEX:52021DC1000.

EEA, F, FOEN, 2020. Is Europe Living Within the Limits of Our Planet? An Assessment of Europe's Environmental Footprints in Relation to Planetary Boundaries, vol. 1. Federal Office of the Environment/European Environmental Agency, Luxembourg, p. 61.

Feranec, J., 2016. Project Corine land cover. In: European Landscape Dynamics. CRC Press, pp. 39–44.

Fernández-Nogueira, D., Corbelle-Rico, E., 2018. Land use changes in Iberian Peninsula 1990–2012. Land 7. https://doi.org/10.3390/land7030099.

Francia Martínez, J.R., Durán Zuazo, V.H., Martínez Raya, A., 2006. Environmental impact from mountainous olive orchards under different soil-management systems (SE Spain). Sci. Total Environ. 358, 46–60. https://doi.org/10.1016/j.scitotenv.2005.05.036.

Franz, G., Pinto, L., Ascione, I., Mateus, M., Fernandes, R., Leitão, P., Neves, R., 2014. Modelling of cohesive sediment dynamics in tidal estuarine systems: case study of Tagus Estuary, Portugal. Estuar. Coast. Shelf Sci. 151, 34–44. https://doi.org/10.1016/j.ecss.2014.09.017.

Giannadaki, D., Giannakis, E., Pozzer, A., Lelieveld, J., 2018. Estimating health and economic benefits of reductions in air pollution from agriculture. Sci. Total Environ. 622, 1304–1316. https://doi.org/10.1016/j.scitotenv.2017.12.064.

Gómez, J.A., Guzmán, M., Giráldez, J.V., Fereres, E., 2009. The influence of cover crops and tillage on water and sediment yield, and on nutrient, and organic matter losses in an olive orchard on a sandy loam soil. Soil Tillage Res. 106, 137–144. https://doi.org/10.1016/j.still.2009.04.008.

Heberger, M., 2023. delineator.py: Fast, Accurate Watershed Delineation Using Hybrid Vector- and Raster-based Methods and Data From MERIT-Hydro. https://doi.org/10.5281/zenodo.10143149.

Lopes, J.F., Lopes, C.L., Dias, J.M., 2019. Climate change impact in the Ria de Aveiro Lagoon ecosystem: a case study. J. Mar. Sci. Eng. 7. https://doi.org/10.3390/jmse7100352.

Neves, V.H., Pace, G., Delegido, J., Antunes, S.C., 2021. Chlorophyll and suspended solids estimation in Portuguese reservoirs (Aguieira and Alqueva) from Sentinel-2 imagery. Water 13. https://doi.org/10.3390/w13182479.

Pacheco, F., Sanches Fernandes, L., 2016. Environmental land use conflicts in catchments: a major cause of amplified nitrate in river water. Sci. Total Environ. 548, 173–188. https://doi.org/10.1016/j.scitotenv.2015.12.155.

Palma, P., Fialho, S., Lima, A., Catarino, A., Costa, M., Barbieri, M., Monllor-Alcaraz, L., Postigo, C., de Alda, M.L., 2021. Occurrence and risk assessment of pesticides in a Mediterranean basin with strong agricultural pressure (Guadiana basin: southern of Portugal). Sci. Total Environ. 794, 148703. https://doi.org/10.1016/j.scitotenv.2021.148703.

Portela, M.M., Espinosa, L.A., Zelenakova, M., 2020. Long-term rainfall trends and their variability in mainland Portugal in the last 106 years. Climate 8 (12), 146. https://doi.org/10.3390/cli8120146. https://www.mdpi.com/2225-1154/8/12/146.

Radbourne, A.D., Ryves, D.B., Madgwick, G., Anderson, N.J., 2020. The influence of climate change on the restoration trajectory of a nutrient-rich deep lake. Ecosystems 23, 859–872. https://doi.org/10.1007/s10021-019-00442-1.

Raposo, A., Mansilha, C., Veber, A., Melo, A., Rodrigues, J., Matias, R., Rebelo, H., Grossinho, J., Cano, M., Almeida, C., Nogueira, I.D., Puskar, L., Schade, U., Jordao, L., 2022. Occurrence of polycyclic aromatic hydrocarbons, microplastics and biofilms in alqueva surface water at touristic spots. Sci. Total Environ. 850, 157983. https://doi.org/10.1016/j.scitotenv.2022.157983.

Rodrigues, G., Potes, M., Costa, M.J., Novais, M.H., Penha, A.M., Salgado, R., Morais, M. M., 2020. Temporal and spatial variations of Secchi depth and diffuse attenuation coefficient from Sentinel-2 MSI over a large reservoir. Remote Sens. 12.

Rodrigues, M., Rosa, A., Cravo, A., Jacob, J., Fortunato, A.B., 2021. Effects of climate change and anthropogenic pressures in the water quality of a coastal lagoon (Ria Formosa, Portugal). Sci. Total Environ. 780, 146311. https://doi.org/10.1016/j.scitotenv.2021.146311.

Santos, J., Corte-real, J., Leite, S., 2007. Atmospheric large-scale dynamics during the 2004/2005 winter drought in Portugal. Int. J. Climatol. 27, 571–586. https://doi.org/10.1002/joc.1425.

Santos, S., Vilar, V.J.P., Alves, P., Boaventura, R.A.R., Botelho, C., 2013. Water quality in Minho/Miño river (Portugal/Spain). Environ. Monit. Assess. 185, 3269–3281.

Schlingmann, M., Tobler, U., Berauer, B., Garcia-Franco, N., Wilfahrt, P., Wiesmeier, M., Jentsch, A., Wolf, B., Kiese, R., Dannenmann, M., 2020. Intensive slurry management and climate change promote nitrogen mining from organic matter-rich montane grassland soils. Plant Soil 456, 81–98. https://doi.org/10.1007/s11104-020-04697-9.

Serpa, D., Ferreira, R., Machado, A., Cerqueira, M., Keizer, J., 2020. Mid-term post-fire losses of nitrogen and phosphorus by overland flow in two contrasting eucalypt stands in North-Central Portugal. Sci. Total Environ. 705, 135843. https://doi.org/10.1016/j.scitotenv.2019.135843.

Silva, E., Pereira, A.C., Estalagem, S.P., Moreira-Santos, M., Ribeiro, R., Cerejeira, M.J., 2012. Assessing the quality of freshwaters in a protected area within the Tagus River Basin District (Central Portugal). J. Environ. Qual. 41, 1413–1426. https://doi.org/10.2134/jeq2012.0010.

Teixeira, P., Costa, S., Brown, B., Silva, S., Rodrigues, R., Valério, E., 2020. Quantitative PCR detection of enteric viruses in wastewater and environmental water sources by the Lisbon municipality: a case study. Water 12. https://doi.org/10.3390/w12020544.

Vale, P., 2023. Impact of drought and wildfires in recent trends of diarrhetic shellfish toxins in cockles from Northwest Portugal and its similarities with sardine stock trends in the period 2001–2022. Estuar. Coasts 46, 1792–1807. https://doi.org/10.1007/s12237-023-01244-4.

Vidal, T., Pereira, J.L., Moreira, F., Silva, J., Santos, M., Campos, I., Benoliel, M.J., Paiva, J.M., Cardoso, V.V., Barreto, R., Neto, A.Q., Gonçalves, F., Abrantes, N., 2021. Responses of benthic diatoms to waters affected by post-fire contamination. Sci. Total Environ. 800, 149473. https://doi.org/10.1016/j.scitotenv.2021.149473.

Vieira, J.M.P., Pinho, J.L.S., Dias, N., Schwanenberg, D., van den Boogaard, H.F.P., 2013. Parameter estimation for eutrophication models in reservoirs. Water Sci. Technol. 68, 319–327. https://doi.org/10.2166/wst.2013.248.

World-Bank, 2024. World Bank open data website. https://data.worldbank.org.

Yamazaki, D., Ikeshima, D., Sosa, J., Bates, P.D., Allen, G.H., Pavelsky, T.M., 2019. Merit hydro: a high-resolution global hydrography map based on latest topography dataset. Water Resour. Res. 55, 5053–5073. https://doi.org/10.1029/2019WR024873.

Zhou, Y., Xu, J., Yin, W., Ai, L., Fang, N., Tan, W., Yan, F., Shi, Z., 2017. Hydrological and environmental controls of the stream nitrate concentration and flux in a small agricultural watershed. J. Hydrol. 545, 355–366. https://doi.org/10.1016/j.jhydrol.2016.12.015.